Rheology of gelatin solutions at the sol-gel transition

J. Peyrelasse,[1] M. Lamarque,[1] J. P. Habas,[1] and N. El Bounia[2]
[1]*Laboratoire de Physique des Matériaux Industriels, URA 1494, Université de Pau, Centre Universitaire de Recherche Scientifique, Avenue de l'Université, 64000 Pau, France*
[2]*Groupement de Recherche de Lacq, Boîte, Postale 34, 64170 Artix, France*
(Received 2 January 1996)

This paper presents the results of rheological measurements of solutions of gelatin in the transition zone preceding the gel temperature. The relaxation function $G(t)$ proposed by Martin, Adolf, and Wilcoxon [Phys. Rev. A **39**, 1325 (1989)] leads to very good agreement between the experimental data [$\eta'(\omega)$ and $\eta''(\omega)$] and the calculated curves. The gel strength and characteristic time are determined as a function of temperature. [S1063-651X(96)00606-X]

PACS number(s): 82.70.Gg, 83.10.−y, 83.80.Lz

I. INTRODUCTION

A gel is a giant polymer made up of molecules that are branched in three dimensions and form a lattice. Gels are commonly classified in two groups: chemical gels and physical gels, which are in fact different essentially through the nature of the bonds linking the molecules together.

If a gel is produced by a chemical reaction, the bonds created are covalent bonds and the gel formed is irreversible. The aggregation mechanisms in the case of physical gels do not lead to the formation of covalent bonds but, on the contrary, to bonds that are reversible when thermodynamic parameters such as pH, ionic strength, or temperature are modified.

For many gels made up of macromolecules of biological origin, the formation of the lattice is achieved by means of a conformational transition from coils to helix. This is the case in the formation of gelatin gels as well as, for example, in polysaccharide gels [1–4].

Different models have been proposed to explain the formation and properties of gels. So-called classical models were put forth by Flory and Stockmayer [5,6]. A branched molecule grows randomly with no constraints and without formation of cycles. This is the Cayley tree or Bethe lattice model. This model has the advantage of providing a complete analytical solution as regards the gel point and many molecular parameters. The second model is a kinetic model known as the kinetic gelation model [7,8].

A more recent model is that proposed by Stauffer Coniglio, and Adam [9,10] and de Gennes [11,12], who noted that the gel transition could be described using the percolation model. This statistical model assumes that the monomers occupy all possible sites in a lattice with a functionality equal to the number of closest neighbors. The bonds are formed randomly with a probability p simulating the fraction of monomers having reacted. When $p<p_c$ only small clusters are formed, whereas if $p>p_c$ an infinite cluster appears corresponding to the formation of a gel. The value of p_c depends on the nature of the lattice and generally cannot be calculated exactly. The merit of this model is that it takes full account of the excluded volume and cyclization effects. On the other hand, it does not generally have an analytical solution and Monte Carlo methods have to be used in order to exploit it [13]. Numerical analysis shows that in the neighborhood of p_c the size and mass of clusters differ widely. The number of clusters of mass M is given by the distribution law

$$n(M)=M^{-\tau}F\left(\frac{M}{M^*}\right). \tag{1}$$

The exponent τ depends on the dimension d of the space, but not on the details of the system studied (the nature of the lattice in particular). $F(x)$ is a cutoff function that truncates the decrease in power law for $M=M^*$. M^* is the mass of the typical cluster, i.e., the cluster that makes a dominant contribution to the value of the moments of an order higher than two in the distribution. An exponential function seems to provide a good approximation for $F(x)$. When p increases, M^* increases and diverges at the percolation threshold according to the law

$$M^*\propto|p-p_c|^{-1/\sigma} \tag{2}$$

in which σ is a second exponent.

The correlation length, which is the radius of gyration of the cluster of mass M^*, also diverges at the percolation threshold

$$\xi\propto|p-p_c|^{-\nu}. \tag{3}$$

$\nu=1/D\sigma$, where D is the fractal dimension.

It is possible with these hypotheses to determine the different moments of the mass distribution. The weight-average molecular weight M_w diverges at the gel point, but the number-average molecular weight M_n does not diverge. Several experimental investigations have shown that connectivity properties are well described by the percolation model [14,15].

The most obvious manifestation of the sol-gel transition concerns mechanical properties. The dynamic viscosity η_0 diverges as the system reaches the gel point. Immediately after this point a zero-frequency elastic modulus G_0 appears.

Like many molecular parameters, η_0 and G_0 follow power laws in the vicinity of the gel point [16–20]

$$\eta_0 \propto |p-p_c|^{-s} \quad \text{if } p<p_c, \tag{4}$$

$$G_0 \propto |p-p_c|^{u} \quad \text{if } p>p_c. \tag{5}$$

In these relationships, p is a parameter characterizing the evolution towards the gel point. In the case of a chemical reaction, p represents the rate of advancement of the reaction. The kinetics leading to gelation are often isothermal and it may be assumed that in the neighborhood of the gel point, the rate of advancement is a linear function of time. In these conditions, p can be replaced in the previous equations by time. For our gelatin solutions, gelation is obtained through variation of temperature. It seems that in this case it is not possible to determine the exponents since the prefactors of the equations are unknown functions of temperature.

As far as dynamic behavior is concerned, a large number of experimental studies [21–26] have shown that the complex shear modulus G^* follows a power law as a function of angular frequency ω:

$$G^* \propto (j\omega)^n, \tag{6}$$

i.e.,

$$G' \propto G'' \propto \omega^n. \tag{7}$$

The loss angle is thus given by

$$\delta = \arctan(G''/G') = n\pi/2. \tag{8}$$

Martin, Adolf, and Wilcoxon [27] conducted a complete theoretical analysis of this phenomenon. The relaxation function obtained is of the form

$$G(t) \propto t^{-[d\nu/(d\nu+s)]}. \tag{9}$$

It should be noted that a relaxation function of the same type was proposed by Winter and Chambon [28,29].

Using a Fourier transform the complex shear modulus can be calculated

$$G^*(\omega) \propto \omega^{[d\nu/(d\nu+s)]}. \tag{10}$$

It will be noted that the results obtained using this model are consistent with the experimental results. The exponent n in the Martin-Adolf-Wilcoxon theory is given by

$$n = \frac{d\nu}{d\nu+s}. \tag{11}$$

It can also be shown, independently of any theory, that if Eqs. (4) and (5) are valid, the exponent n is closely linked to the exponents characterizing viscosity η_0 and the zero-frequency elastic modulus G_0:

$$n = \frac{u}{s+u}. \tag{12}$$

In the framework of the analysis proposed by Martin, Adolf, and Wilcoxon $u = d\nu$.

Knowledge of the values of exponents s,u,n is of major importance. Data currently available in the literature show a certain confusion. As regards the values of n, it is apparently now accepted that a wide variety of values can be obtained experimentally [30–32]. Scalan and Winter, in particular, have shown that n depends not only on the stoechiometric ratio r but also on the initial molar mass of the monomers and on their concentration when the reaction takes place in a solution. In the case of cross linking of poly(dimethylsiloxane) by a tetrafunctional cross-linking agent, they obtain values varying from 0.2 to 0.92 depending on the experimental conditions. These experimental results seem to show that there is no universal value of n, although certain theories predict a precise value of this exponent for all gels [27,33,34].

It can therefore be noted that the theoretical problem posed by the value of exponents involved in viscoelastic properties is still an open question. The disparity observed in experimental results is perhaps due to the fact that the fractal dimension of the clusters is not universal but depends on the environment in which they evolve [35,36].

II. EXPERIMENTAL CONDITIONS

We conducted a study of the rheological properties in a dynamic regime of gelatin solutions as a function of temperature. These studies were carried out using a Rheometrics dynamic stress rheometer working with imposed strain. We used a Couette-type geometry and sinusoidal periodic shearing. The angular frequency domain used varied from 10^{-1} to 10^2 rad s^{-1}. The torque sensor available can only measure torques higher than 0.2 g cm.

The gelatin samples were supplied by Systems Bio-Industries. They were limed ossein extracts of weight-average molecular weight $M_w = 295\,000$ g mol^{-1} and gel temperature $T_g = 36$ °C. The solutions were prepared in distilled water. An antibacterial agent was systematically added. Unlike most of the studies carried out before this one, our solutions were not quenched but were progressively cooled from 60 °C down to the gelation temperature T_g. A previous study [37] shows that at the highest temperatures, viscosity and optical rotation do not change with time. On the other hand, a few degrees above the gel point an increase with time in both viscosity and optical rotation can be observed. These kinetics reflect the progressive formation of the lattice, which is a kinetic process. At each temperature a state of equilibrium is of course achieved (constancy of viscosity and optical rotation), characteristic of a stationary mass distribution of clusters. The measurements presented in this paper were, in all cases, taken when such an equilibrium was reached.

III. EXPERIMENTAL RESULTS

Figures 1 and 2 present the storage and loss modulus curves $G'(\omega)$ and $G''(\omega)$ in logarithmic scale. The concentration of the solution is $C = 0.28$ g cm^{-3}.

It will be seen that at the highest temperatures G' is proportional to ω^2 and G'' to ω over a large frequency domain. On the basis of their definitions it is thus possible to determine the viscosity η_0 as well as the creep compliance J_e^0:

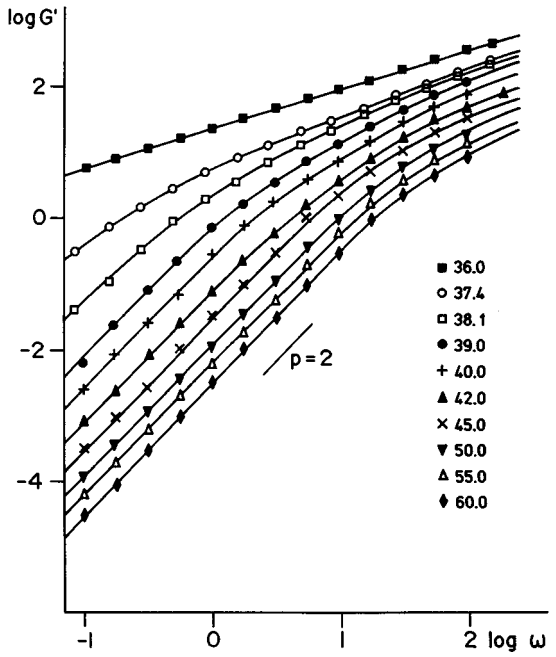

FIG. 1. Storage modulus G' (Pa) as a function of the shear angular frequency ω (rad s^{-1}), shown at different temperatures (in °C). The x,y axes are expressed in decimal logarithmic scale.

$$J_e^0=\frac{1}{\eta_0^2}\lim_{\omega\to 0}\frac{G'}{\omega^2},\quad \eta_0=\lim_{\omega\to 0}\frac{G''}{\omega}. \tag{13}$$

If $\omega\to 0$,

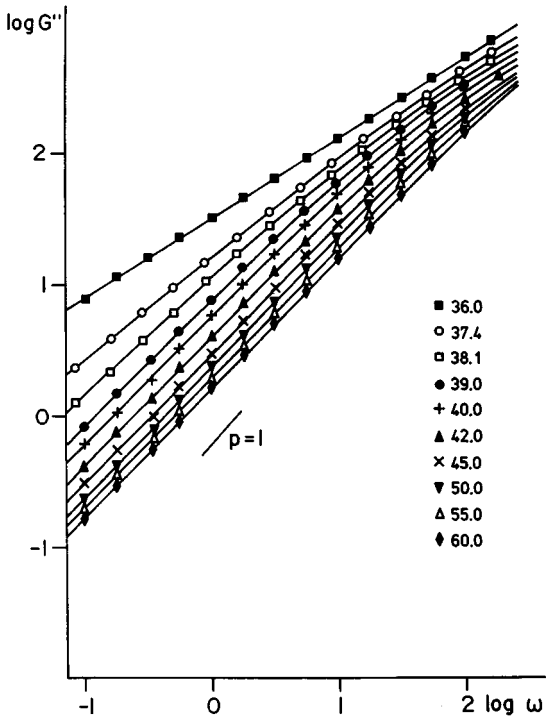

FIG. 2. Loss modulus G'' (Pa) as a function of the shear angular frequency ω (rad s^{-1}), shown at different temperatures (in °C). The x,y axes are expressed in decimal logarithmic scale.

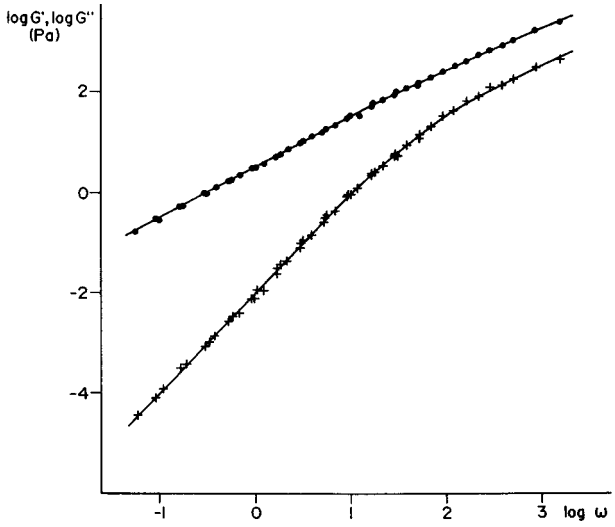

FIG. 3. Master curves $G'(\omega)$ and $G''(\omega)$. The time-temperature superposition is for 39 °C$<T<$60 °C. The x,y axes are expressed in decimal logarithmic scale.

$$\log_{10}(G')=\log_{10}(J_e^0\eta_0^2)+2\log_{10}(\omega), \tag{14}$$

$$\log_{10}(G'')=\log_{10}(\eta_0)+\log_{10}(\omega),$$

Numerical analysis of the straight lines $\log_{10}(G')$ and $\log_{10}(G'')$ as a function of $\log_{10}(\omega)$ leads directly to values of η_0 and then J_e^0.

When the temperature decreases it can be seen that the frequency range in which G' and G'' are respectively proportional to ω^2 and ω decreases. Finally, for $T=36$ °C the curves $\log_{10}(G')$ and $\log_{10}(G'')$ versus $\log_{10}(\omega)$ are straight lines with the same slope throughout the domain of accessible frequencies. This temperature corresponds to the gel point.

The $G^*(\omega)$ master curves in Fig. 3 have been obtained using time-temperature superposition in the temperature range 39 °C–60 °C. In this temperature range no evolution of viscosity or optical rotation with time can be observed. It can therefore be considered that the gelation process has not begun at these temperatures. These curves reveal no rubbery plateau and thus the molecules of gelatin in solution do not appear to be entangled.

To analyze the results at intermediate temperatures, it is preferable to plot $\eta''=f(\eta')$ curves. This representation is known as the Cole-Cole diagram. Figure 4 displays the results obtained at different temperatures. In this representation a straight line is obtained at the gel point running through the origin and having a slope equal to $\cot(n\pi/2)$.

IV. ANALYSIS OF THE RESULTS

If we are somewhat beneath the gel point, the decay of $G(t)$ will no longer be a power law. Friedrich, Heymann, and Berger [38] have proposed empirically a relaxation function to represent the rheological behavior of systems evolving towards the gel point. This function is written

$$G(t)=St^{-k}e^{-t/\tau_0}, \tag{15}$$

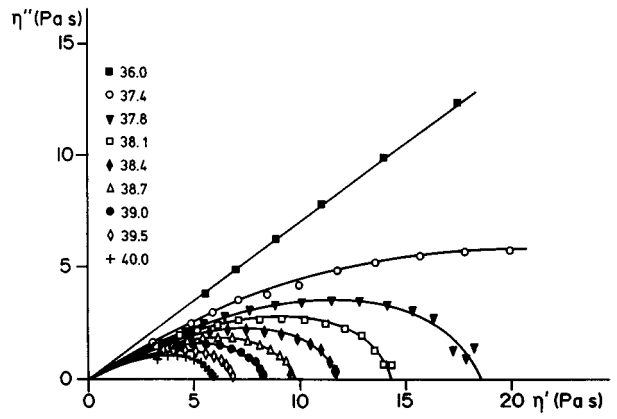

FIG. 4. Cole-Cole plot η'' (Pa s) versus η' (Pa s).

in which τ_0 is a time constant and S a quantity, which will be defined below. It is clear that the quantities τ_0, S, k will depend on the ''distance'' from the gel point, i.e., in the case of gelatin solutions, on the temperature.

The advantage of the Friedrich-Heymann-Berger function with respect to that proposed by Winter and Chambon [28,29] would be its ability to describe the rheological behavior not only in the immediate vicinity of the gel point but also throughout the transition zone preceding the gel point. However, it is important to note that the two relaxation functions coincide close to the gel point. If $\tau_0 \to \infty$, $k \to n$, $S \to S_g$, and therefore $G(t) = S_g t^{-n}$. S_g is the gel strength defined by Winter and Chambon.

Unlike Friedrich, Heymann, and Berger, who worked on the function $G^*(\omega)$, we preferred to calculate $\eta^*(\omega)$. By definition,

$$\eta^*(\omega) = \int_0^\infty G(t) e^{-j\omega t} dt = \frac{S\tau_0^{1-k}\Gamma(1-k)}{(1+j\omega\tau_0)^{1-k}}. \tag{16}$$

Γ represents the usual gamma function. It can be observed that $S\tau_0^{1-k}\Gamma(1-k)$ represents the viscosity η_0 [limit of $\eta^*(\omega)$ when $\omega \to 0$]. So for complex viscosity one obtains

$$\eta^*(\omega) = \frac{\eta_0}{(1+j\omega\tau_0)^{1-k}}. \tag{17}$$

The reader may have recognized the well-known Davidson-Cole relationship. This relationship has been widely used by dielectricians.

A nonlinear regression program was used to determine the best values of the three parameters η_0, τ_0, and k. In Fig. 5 we have reported as an example the best curve $\eta''(\omega)$ compared with the data. ($T = 37.8$ °C.) The fit is seen to be unsatisfactory.

On the other hand, Martin, Adolf, and Wilcoxon [39], show that at long times $t > \tau_0$ only the exponentially rare clusters, with $M \gg M^*$ will still contribute to the decay of $G(t)$. These clusters are lattice animals with fractal dimension $D_S = 2$. The long-time tail of $G(t)$ may be described by the relaxation of Zimm modes of exponentially distributed lattice animals. Summing over the discrete internal modes of a single lattice animal and then averaging over the distribution of cluster size, they obtain, for the long time tail,

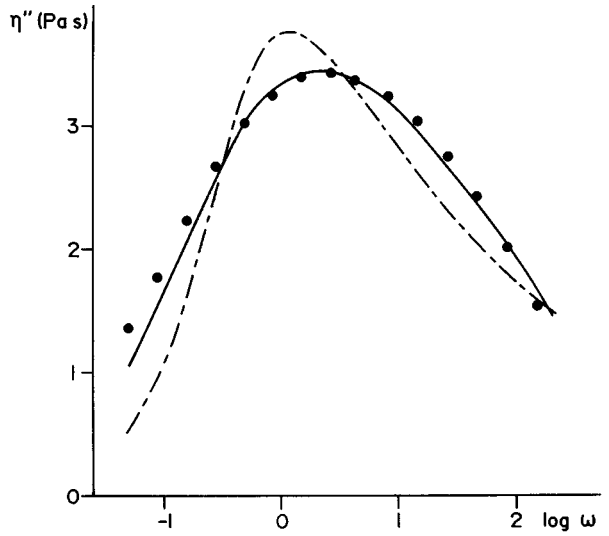

FIG. 5. η'' (Pa s) versus angular frequency ω (rad s^{-1}) at $T = 37.8$ °C: ●●●, experimental points; ----, curve fitting with the Friedrich-Heymann-Berger relaxation function; —, curve fitting with the Martin-Adolf-Wilcoxon function.

$$G(t) \propto e^{-(t/\tau_0)^\beta}, \quad \beta = \frac{D_S}{D_S + d} = \frac{2}{5}. \tag{18}$$

Although it cannot be rigorously justified, Martin, Adolf, and Wilcoxon propose a useful form of $G(t)$ for fitting the data:

$$G(t) = St^{-k} e^{-(t/\tau_0)^\beta}. \tag{19}$$

Close to the gel point ($\tau_0 \to \infty$, $S \to S_g$, $k \to n$) one once again finds $G(t) = S_g t^{-n}$ and the complex elastic modulus is thus given by $G^* \propto (j\omega)^n$.

Martin, Adolf, and Wilcoxon's relaxation function cannot provide a simple analytical form for $G^*(\omega)$ or for $\eta^*(\omega)$ as was the case with the Friedrich function. However, one can calculate the limits values when $\omega \to 0$:

$$\lim_{\omega \to 0} \eta' = \eta_0 = S \frac{\tau_0^{1-k}}{\beta} \Gamma\left(\frac{1-k}{\beta}\right). \tag{20}$$

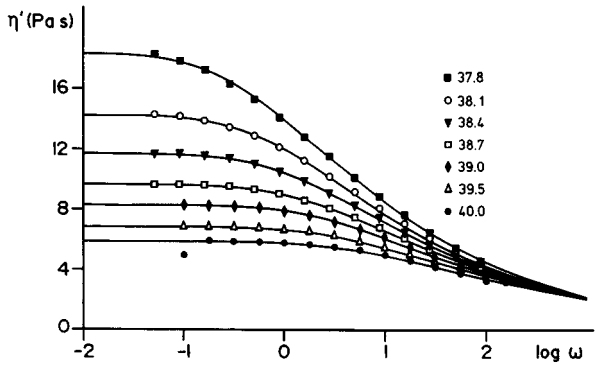

FIG. 6. η' (Pa s) versus angular frequency ω (rad s^{-1}) at different temperatures. The solid curves represent calculated values with the parameters given in Table I (the Martin-Adolf-Wilcoxon model).

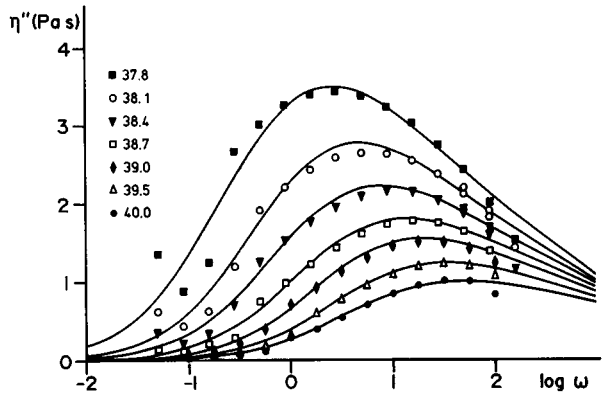

FIG. 7. η'' (Pa s) versus angular frequency ω (rad s^{-1}) at different temperatures. The solid curves represent calculated values with the parameters given in Table I (the Martin-Adolf-Wilcoxon model).

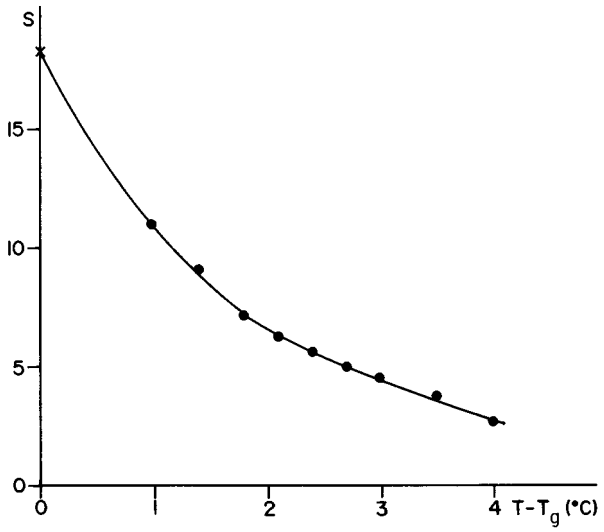

FIG. 8. Variations of the gel strength S versus $T-T_g$ in °C. T_g is the gel temperature: $\times$ is the value of S_g calculated with Eq. (23). (If $T\rightarrow T_g$, then $S\rightarrow S_g$.)

As $G^*=j\omega\eta^*$ one obtains $G''\propto\omega$ if $\omega\rightarrow 0$. Similarly,

$$\lim_{\omega\rightarrow 0}\ \eta''=S\omega\ \frac{\tau_0^{2-k}}{\beta}\ \Gamma\left(\frac{2-k}{\beta}\right). \tag{21}$$

One also obtains $G'\propto\omega^2$ if $\omega\rightarrow 0$. The expression of the creep compliance can be deduced from the previous result:

$$J_e^0=\frac{\beta}{S}\ \tau_0^k\ \frac{\Gamma\left(\frac{2-k}{\beta}\right)}{\Gamma^2\left(\frac{1-k}{\beta}\right)}. \tag{22}$$

So the only way to obtain η^* from $G(t)$ is to calculate the Fourier transform numerically. Great care is necessary in carrying out the calculations. In particular the function $G(t)$ must be digitized over a very large time interval. Moreover, as the functions $G(t)\sin(\omega t)$ and $G(t)\cos(\omega t)$ oscillate very rapidly when ω is large, a very large number of points are necessary to define them correctly. Let us indicate that for $\omega=0$ it is possible to verify the accuracy of the numerical calculation since the results can also be obtained by means of the analytical form [Eq. (20)].

We developed a nonlinear regression program able to determine the best values of S,τ_0,β,k. It can be seen in Fig. 5 that the Martin-Adolf-Wilcoxon law yields better results than the Friedrich-Heymann-Berger law. Figures 6 and 7 show that we obtain very good agreement between the experimental data [$\eta'(\omega)$ and $\eta''(\omega)$] and the calculated curves.

The parameters S,k,β,τ_0 are given in Table I. This table has been completed with values of η_0 and then J_e^0 either determined directly from the $G'(\omega)$ or $G''(\omega)$ curves [Eq.

TABLE I. Best values of S, τ_0, β, and k calculated by curve fitting (the Martin-Adolf-Wilcoxon model). The asterisks denote η_0 and J_e^0 determined directly from the $G'(\omega)$ and $G''(\omega)$ curves [Eq. (14)]. The other values are calculated with Eqs. (20) and (22).

T (°C)	S	η_0 (Pa s)	J_e^0 (10^{-3} Pa^{-1})	τ_0 (10^{-2} s)	β	k
60		1.71*	1.15*			
55		2.0*	1.4*			
50		2.4*	1.8*			
45		3.1*	2.5*			
42		4.0*	4.8*			
40	3.2	5.9	10.1	5.4	0.433	0.760
39.5	3.9	6.9	10.8	7.4	0.458	0.743
39	4.5	8.2	14.1	11.2	0.464	0.730
38.7	5.0	9.7	18.6	15.1	0.448	0.725
38.4	5.6	11.6	26.9	23.0	0.439	0.714
38.1	6.2	14.3	33.3	38.1	0.455	0.706
37.8	7.1	18.4	54.9	58	0.418	0.701
37.4	9.2	28.6	84.3	127	0.420	0.680
37.0	11.1	59.5	196	740	0.450	0.665
36.0	18.6					0.620

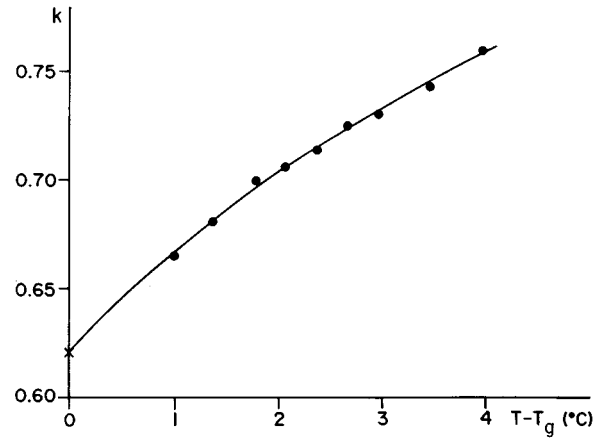

FIG. 9. Variations of k versus $T-T_g$ in °C. T_g is the gel temperature: $\times$ is the value of n calculated with Eq. (23). (If $T\rightarrow T_g$, then $k\rightarrow n$.)

(14)] or calculated from relationships (20) and (22).

We can see that β is nearly a constant. The mean value obtained is 0.44, which is in accordance with the Martin-Adolf-Wilcoxon predictions ($\beta=0.4$).

We have reported in Figs. 8 and 9 the variations of S and k versus temperature. Figures 10–12 display variations of η_0, J_e^0, and τ_0 as a function of temperature. It can be seen that these three quantities diverge at the gel point. However, it is not possible to determine the corresponding critical exponents since the prefactors are unknown functions of temperature.

As we have already pointed out, at the gel point the relaxation function is given by $G(t)=S_g t^{-n}$. After the Fourier

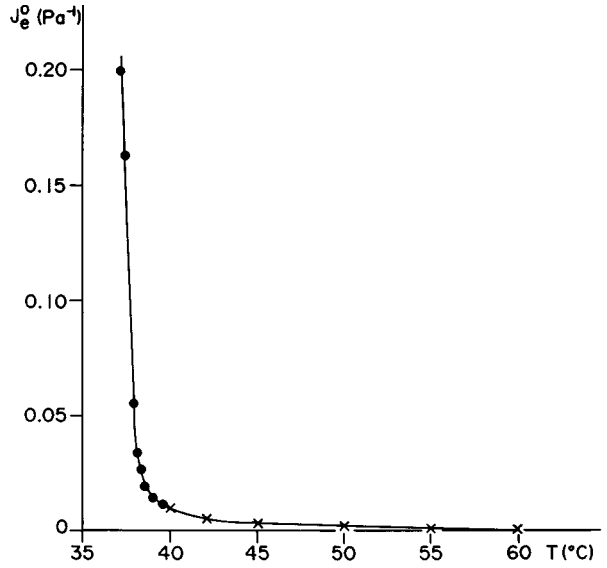

FIG. 11. Increase of the creep compliance J_e^0 (Pa^{-1}) when the temperature is close to the gel temperature: $\times$, calculated with Eq. (14); ●, calculated with Eq. (22).

transform the following variations of G' and G'' versus ω are obtained:

$$G'=S_g\Gamma(1-n)\cos(n\pi/2)\omega^n,$$

$$G''=S_g\Gamma(1-n)\sin(n\pi/2)\omega^n. \tag{23}$$

The loss angle δ is given by $\delta=n\pi/2$. $\tan(\delta)$ is independent of ω. This observation is used to determine reliably both

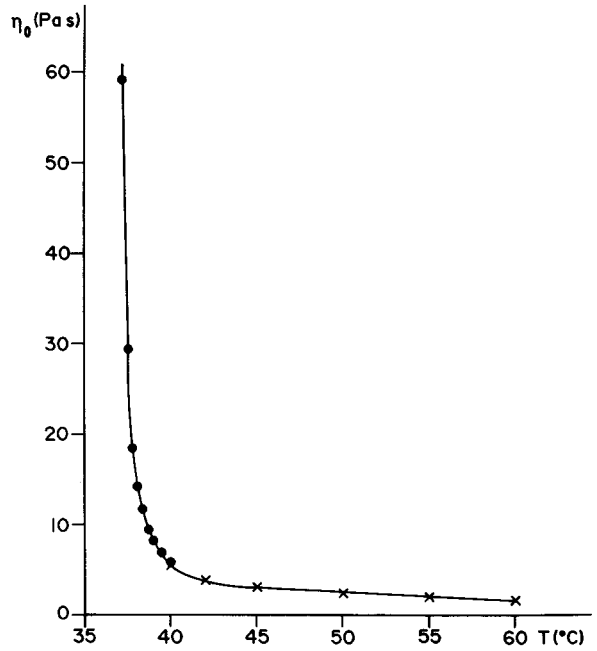

FIG. 10. Increase of viscosity η_0 (Pa s) when the temperature is close to the gel temperature: $\times$, calculated with Eq. (14); ●, calculated with Eq. (20).

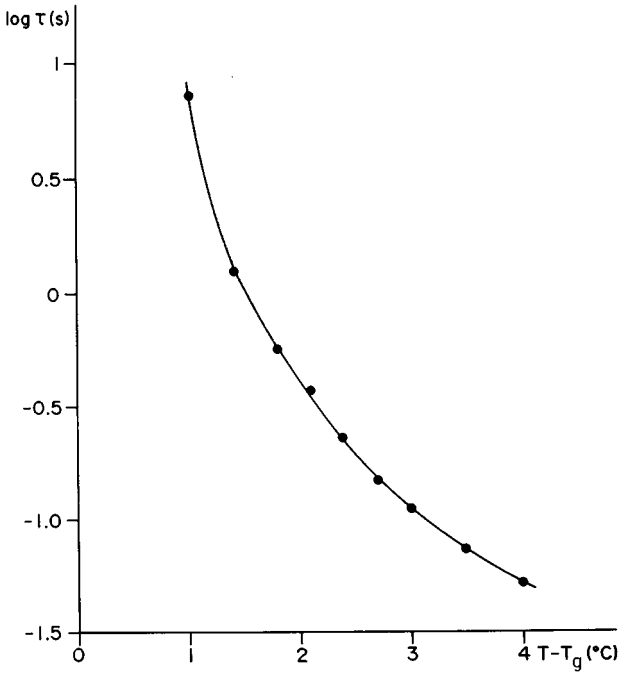

FIG. 12. Increase of the characteristic time τ_0 (s) when the temperature is close to the gel temperature. The y axis is expressed in decimal logarithmic scale.

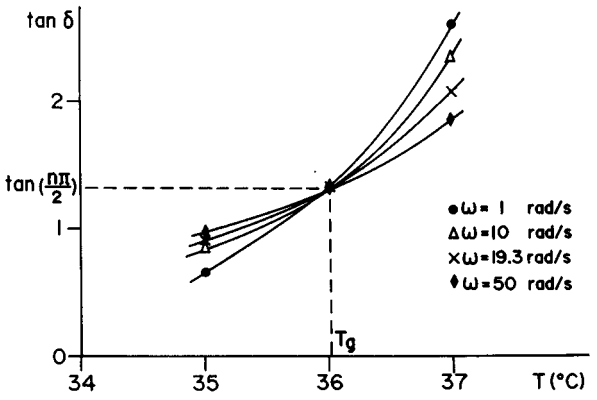

FIG. 13. tan(δ) as a function of temperature (in °C) is shown at various frequencies, along with the determination of the gel temperature T_g and the critical exponent n.

the gelation temperature and the value of n at the gel point. If variations of tan(δ) versus temperature are plotted at various frequencies, one should obtain curves that intersect at T_g. The value of the y axis at this point can be used to obtain n. This method is useful when the gel point is not known accurately or when the measurements have not been carried out rigorously at T_g. Figure 13 gives an example of this determination.

When the determinations of G' and G'' are conducted rigorously at the gel point, the curves $G'(\omega)$ and $G''(\omega)$ (on a log-log scale) are straight lines throughout the domain of accessible frequencies. This is the case in the example given in Fig. 14. An analysis of these straight lines can also be used to determine n, as well as the value of S_g [Eq. (23)]. The values of S_g and n obtained by this means are positioned satisfactorily on the curves giving variations of S and k versus temperature (Figs. 8 and 9). The exponent n obtained when the concentration is varied (between 0.17 and 0.40 g cm^{-3}) is almost a constant, with mean value $n=0.62$.

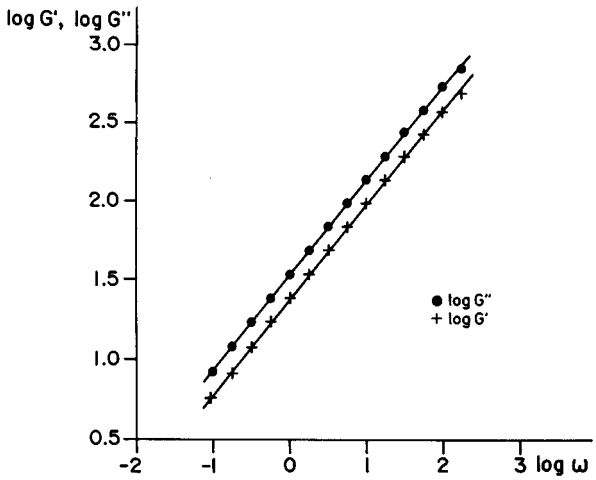

FIG. 14. log-log plot of the frequency dependence of the storage modulus G' (Pa) and loss modulus G'' (Pa) at the gel temperature, along with the determination of S_g and n, calculated with Eq. (23). The x,y axes are expressed in decimal logarithmic scale.

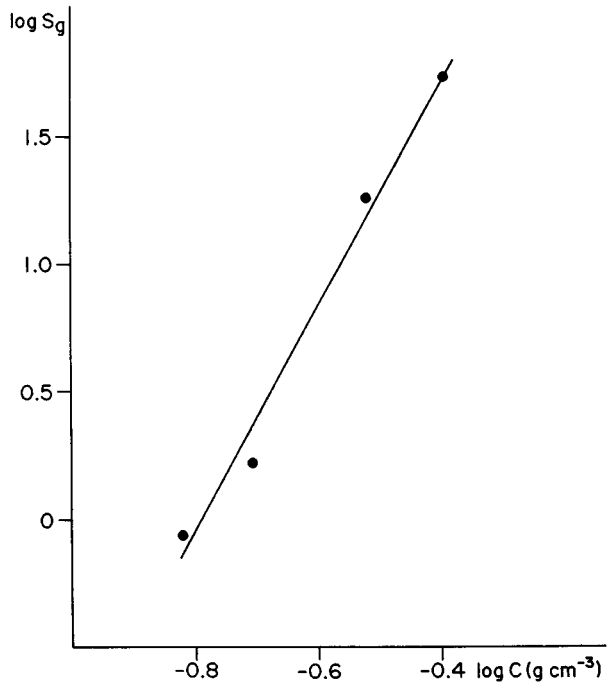

FIG. 15. Variations of the gel strength S_g versus concentration C (in g cm^{-3}). The slope of the straight line is 4.5. The x,y axes are expressed in decimal logarithmic scale.

Finally, let us recall that according to Scalan and Winter [30], S_g follows a law of the type

$$S_g = AC^{-t}. \tag{24}$$

For our gelatin solutions, Eq. (24) appears to be verified as shown in Fig. 15. The slope obtained is equal to 4.5, which is consistent with Scalan and Winter's results.

V. CONCLUSION

We conducted a complete study of the rheological properties in a dynamic regime of gelatin solutions as a function of temperature. This study enabled us to verify that gelatin solutions behaved like classical polymer solutions at high temperatures. For low values of the shearing frequency, the moduli G' and G'' are proportional to ω^2 and ω.

The master curves representing the values of G' and G'' versus ω show no rubbery plateau. This important result seems to indicate that the gelatin molecules in relatively concentrated solutions are not in an entangled regime.

In the vicinity of the gel point, Martin, Adolf, and Wilcoxon's relaxation function $G(t)$ provides a very good fit with experimental results. The gel strength and characteristic time are determined in the whole transition zone preceding the gel point.

At the gel point we verify that the moduli G' and G'' are proportional to ω^n. The value of n obtained does not depend on the concentration of the gelatin solution.

ACKNOWLEDGMENTS

This work was supported by Systems Bio Industries, France. M.L. acknowledges gratefully the ''Conseil Régional d'Aquitaine'' for a research grant.

[1] W. F. Harrington and N. V. Rao, Biochemistry **9**, 3714 (1970).
[2] S. B. Ross-Murphy, Polymer **33**, 2622 (1992).
[3] M. Djabourov and P. Papon, Polymer **24**, 537 (1983).
[4] M. Djabourov, Polym. Inter. **25**, 135 (1991).
[5] P. J. Flory, *Principles of Polymer Chemistry* (Cornell University Press, Ithaca, 1953).
[6] W. H. Stockmayer, J. Chem. Phys. **11**, 45 (1943).
[7] H. J. Herrmann, D. P. Landau, and D. Stauffer, Phys. Rev. Lett. **49**, 412 (1982).
[8] R. M. Ziff, in *Kinetics of Aggregation and Gelation*, edited by F. Family and D. Landau (North-Holland, Amsterdam, 1984), p. 191.
[9] D. Stauffer, *Introduction to Percolation Theory* (Taylor and Francis, London, 1985).
[10] D. Stauffer, A. Coniglio, and M. Adam, Adv. Polym. Sci. **44**, 103 (1982).
[11] P. G. de Gennes, *Scaling Concepts in Polymer Physics* (Cornell University Press, Ithaca, 1979).
[12] P. G. de Gennes, J. Phys. (Paris) Colloq. **4**, C3-17 (1980).
[13] D. Lairez, D. Durand, and J. R. Emery, J. Phys. (France) II **1**, 977 (1991).
[14] M. Adam and M. Delsanti, Contemp. Phys. **30**, 203 (1983).
[15] M. Adam, M. Delsanti, J. P. Munch, and D. Durand, Physica, **163**, 85 (1990).
[16] B. Gauthier Manuel and E. Guyon, J. Phys. (Paris) **41**, L503 (1980).
[17] M. A. V. Axelos and M. Kolb, Phys. Rev. Lett. **64**, 1457 (1990).
[18] Y. Wang, Q. Z. Zang, M. Konno, and S. Saito, Chem. Phys. Lett. **186**, 463 (1991).
[19] M. Adam and J. P. Aime, J. Phys. France II **1**, 1277 (1991).
[20] M. Djabourov, J. Leblond, and P. Papon, J. Phys. (Paris) **49**, 333 (1988).
[21] D. Duran, M. Delsanti, M. Adam, and J. M. Luck, Europhys. Lett. **3**, 97 (1987).
[22] Y. G. Lin, D. T. Mallin, J. C. V. Chien, and H. H. Winter, Macromolecules **24**, 850 (1991).
[23] E. J. Amis, D. F. Hodgson, and Q. Yu, Polym. Prep. **32**, 447 (1991).
[24] P. Matricardi, M. Dentini, and V. Crescenzi, Macromolecules **26**, 4386 (1993).
[25] C. Michon, G. Cuvelier, and B. Launay, Rheol. Acta **32**, 94 (1993).
[26] M. Takahashi, K. Yokoyama, and T. Masuda, J. Chem. Phys. **101**, 798 (1994).
[27] J. E. Martin, D. Adolf, and J. P. Wilcoxon, Phys. Rev. Lett **61**, 2620 (1988).
[28] H. H. Winter and F. Chambon, J. Rheol. **30**, 367 (1986).
[29] F. Chambon and H. H. Winter, J. Rheol. **31**, 683 (1987).
[30] C. Scalan and H. H. Winter, Macromolecules **24**, 47 (1991).
[31] R. Muller, E. Gerard, P. Dugand, P. Rempp, and Y. Gnanou, Macromolecules **24**, 1321 (1991).
[32] A. Isuka, H. H. Winter, and T. Hashimoto, Macromolecules **25**, 2422 (1992).
[33] M. Daoud, J. Phys. A **21**, L237 (1988).
[34] M. Daoud and A. Lapp, J. Phys. Condens. Matter **2**, 4021 (1990).
[35] M. Mathukumar, Macromolecules **22**, 4658 (1989).
[36] C. W. Nan and D. M. Smith, Mater. Sci. Eng. B **10**, L1 (1991).
[37] M. Lamarque and J. Peyrelasse (unpublished).
[38] C. Friedrich, L. Heymann, and H. R. Berger, Rheol. Acta **28**, 535 (1989).
[39] J. E. Martin, D. Adolf, and J. P. Wilcoxon, Phys. Rev. A **39**, 1325 (1989).